

# TURBULENT ENERGY PREDICTION FOR AN EXTERNAL FLOW AROUND VALEO COOLING FAN BY $V^2$ -F MODELLING AND IMPROVED K- $\epsilon$ LOW REYNOLDS MODEL

Nasreddine Akermi <sup>\*1</sup>, Azzeddine Khorsi <sup>†1</sup> and Omar Imine <sup>‡1</sup>

<sup>1</sup> University of Science and Technology of Oran Mohamed-Boudiaf, Oran, Algeria.

## Résumé

Le champ de bruit peut être défini comme étant la conséquence des fluctuations de pression générées par les écoulements turbulents proches des parois solides, qui sont régies par des conversions acoustiques basées sur la théorie de Lighthill. Cet article discute des différents résultats de la simulation numérique pour un écoulement externe autour d'un profil d'aile asymétrique (Valeo CD). La simulation numérique consiste à comparer le modèle  $V^2$ -f original de Durbin et le modèle k- $\epsilon$  à bas Reynolds. Des modifications ont été introduites dans le modèle k- $\epsilon$  standard, en remplaçant le terme de taux de déformation par la vorticit , afin d'am liorer la pr diction d' nergie turbulente du mod le visqueux   faible Reynolds. La comparaison des r sultats obtenus a  t  faite avec des exp riences compl tes dans une grande soufflerie   l' cole centrale de Lyon, et une simulation   grandes  chelles (SGE). Le mod le  $V^2$ -f a montr  une adaptation raisonnable au niveau des zones de s paration et une pr diction satisfaisante d' nergie turbulente pr s de la paroi, ainsi que le mod le k- $\epsilon$  modifi . Les am liorations sont dues aux fluctuations de vitesse normales  $v^2$  et aux effets anisotropiques mod lis s par la fonction de relaxation elliptique proche de la paroi solide.

**Mots clefs:** Valeo CD, STAR-CD, k- $\epsilon$ - bas Reynolds-  $V^2$ -f, Kato-Launder-SGE.

## Abstract

The noise field can be defined as the consequence of pressure fluctuations generated by turbulent flows, close to solid walls, which are governed by acoustics conversions and basing on the Lighthill's theory. This paper is discussing the different results of numerical simulation for an external flow around an asymmetric wing profile (Valeo CD). The Numerical simulation consists of comparing the original Durbin  $V^2$ -f and the k- $\epsilon$  low Reynolds models. Some modifications have been introduced to the k- $\epsilon$  model, by replacing the strain rate term and the vorticity, in order to improve the turbulent energy prediction of the low Reynolds viscous models. The comparison of the results obtained has been made with full experiments in large wind tunnel at the central school of Lyon, and LES simulation. The  $V^2$ -f model has shown a reasonable adaptation to the separation zones and satisfactory turbulent energy prediction near the wall, comparing to the k- $\epsilon$  modified model. The improvements were due to the normal velocity fluctuations  $v^2$ , and the anisotropic effects modelled by the elliptic relaxation function close to the solid wall.

**Keywords:** Valeo CD, STAR-CD, k- $\epsilon$ -low Reynolds-  $V^2$ -f, Kato-Launder-LES.

## 1 Introduction

The high energetic demands are imposing a wide range of researches in order to develop the aerodynamic performances, for the wind turbines design [1], applied to wind energies sources [2], as well as, the cooling fans systems applied to CPU thermo-regulator [1-2].

Additionally, the far field noise, which is a consequence of the pressure fluctuations, generated in turbulent flows and governed by the Lighthill's acoustic analogy [3-4-5].

The numerical investigation of several viscous models is basing on the turbulent kinetic energy prediction near the solid wall [6-7]. The  $V^2$ -f model has been considered for a long period, as a perfect modeling, among the available low Reynolds viscous models [8-9], taking into account the normal velocity scaling, as well as, the singularity near the

wall, however, its weakness appears for the turbulent energy prediction [10-11], which made it, particularly, limited because of its isotropic relaxation function.

In order to improve the near wall mesh quality, the skewed hexahedral elements have been checked basing on the boundary layer refinement, and the normal distance to the wall  $y^+$ . The comparison of these models [12-16] has been made in aim to evaluate the turbulent energy prediction at the flow wake zone with the  $V^2$ -f modelling. The stability of this model has been checked by different turbulent Intensities at the inlet flow.

The fluctuations of the turbulent boundary layers and wake generated around the profile and their interaction with it, particularly near the trailing-edge region, called self-noise or trailing edge noise [17].

In most cases, the fluctuating field is generated from the stationary RANS solution. Turbulence model is used to obtain a stationary solution of the flow

The modifications introduced to the k- $\epsilon$  low Reynolds model are not very popular though and rarely used with the

\* nasreddine\_akermi@yahoo.fr

† azzeddine\_khorsiyahoo.fr

‡ imine\_omar@yahoo.fr

intention of combining the best of both sides implemented to the term of turbulent production between the vorticity and

## 2 The Durbin V<sup>2</sup>-f model equations

The original turbulence model V<sup>2</sup>-f developed by the Professor Durbin (NASA 1991) [8-9]. Due to the modifications introduced to the turbulent energy production, this model becomes transient between turbulent viscosity models and second-order modeling. Most important characteristic of this model is the transport equation for the V<sup>2</sup>-f component that replaces an equations system for the Reynolds tensor components, and additional equation for the scalar function  $f$  added to the energy distribution in equation (2), the flow is assuming isotropic close to the wall.

$$\frac{Dk}{Dt} = \frac{\partial k}{\partial t} + U_j \nabla^j k = P_k - \varepsilon + \nabla^j \left[ \left( v + \frac{v_t}{\sigma_k} \right) \nabla_j k \right] \quad (1)$$

$$\frac{D\varepsilon}{Dt} = \frac{\partial \varepsilon}{\partial t} + U_j \nabla^j \varepsilon = \frac{C_{\varepsilon 1} P_k - C_{\varepsilon 2} \varepsilon}{T} + \nabla^j \left[ \left( v + \frac{v_t}{\sigma_\varepsilon} \right) \nabla_j \varepsilon \right]$$

$$\frac{Dv^{-2}}{Dt} = \frac{\partial v^{-2}}{\partial t} + U_j \nabla^j v^{-2} = k f v^{-2} \frac{\varepsilon}{k} + \nabla^j \left[ \left( v + \frac{v_t}{\sigma_k} \right) \nabla_j v^{-2} \right] \quad (2)$$

$$L^2 \nabla^2 f - f = \frac{1}{T} (C_1 - 1) \left[ \frac{v^{-2}}{k} - \frac{2}{3} \right] - C_2 \frac{P_k}{k} \quad (3)$$

For the homogeneous flow zones ( $\nabla^2 f = 0$ ) (isotropic production), the time and the turbulent length given by:

$$T = \max \left[ \frac{k}{\varepsilon}, 6 \sqrt{\frac{v}{\varepsilon}} \right], \text{ and} \quad (4)$$

$$L = C_L \max \left[ \frac{k^{3/2}}{\varepsilon}, C_\eta \frac{v^{3/4}}{\varepsilon^{1/4}} \right]$$

Constants of the model:

$$\begin{aligned} C_\mu &= 0.19, k = 1, \varepsilon = 1.3 \\ C_{\varepsilon 2} &= 1.9, C_1 = 1.4, C_L = 0.3, C_\eta = 70 \\ C_{\varepsilon 1} &= 1.4 \cdot \left[ 1 + 0.045 \sqrt{\frac{k}{v^{-2}}} \right] \end{aligned} \quad (5)$$

## 3 Problem solution

The first step is studying an asymmetric airfoil with controlled diffusion "Valeo CD" for low Reynolds number, applied in automotive motorization, and processors cooling by Valeo fans design, corresponding to the experiences carried out in the wind tunnels at Central school of Lyon, which provides the reference of the experimental data basis. The present case corresponds to a pitch angle of 8° and mean velocity inlet of 16 m/s (a Reynolds number of  $1.2 \times 10^5$  basing on the chord length dimension). The symmetry condition is applied to the top and the bottom of the domain boundaries.

## 4 Boundary conditions

The set of generated meshes insure the validation method, which release the relationship between the meshes quality and the experimental results, a prior, for asymmetric airfoil simulation [4].

This mesh has been generated by Gambit software in "two dimensions", and exported to the PRO-STAR software in order to control the boundary conditions of the mesh, which is extruded in three dimensions" to run the simulation using the STAR-CD (CCM+) code.

A mesh generated taking in account the geometry coordinates (the chord length  $C=1$ ), and the numerical workspace, one time of the chord at the inlet flow  $1 \times C$  (Inlet velocity profile) and two times of the chord at the outlet flow  $2 \times C$ ,  $1.5 \times C$  in the top and  $1.5 \times C$  at the bottom,. The boundary conditions represented in Figure 1.

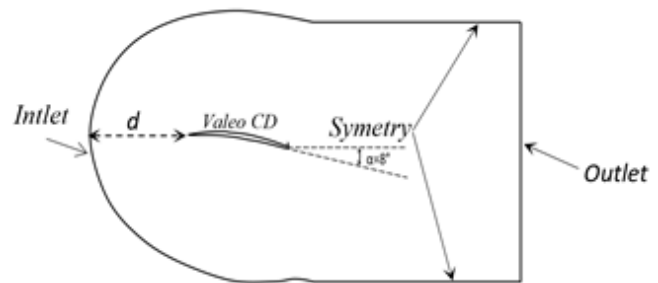


Figure 1: Calculation domain with Boundary conditions

The mesh quality represents the most important stability factor of results. Different meshes sizes have been tested to control the independency of results, in the present simulation a mesh of 86000 cells (Figure 2) has been exploited insuring a normal distance to the wall  $y^+$  lower than 0.35, this mesh is refined too much near the wall in aim to insure a best mesh validation.

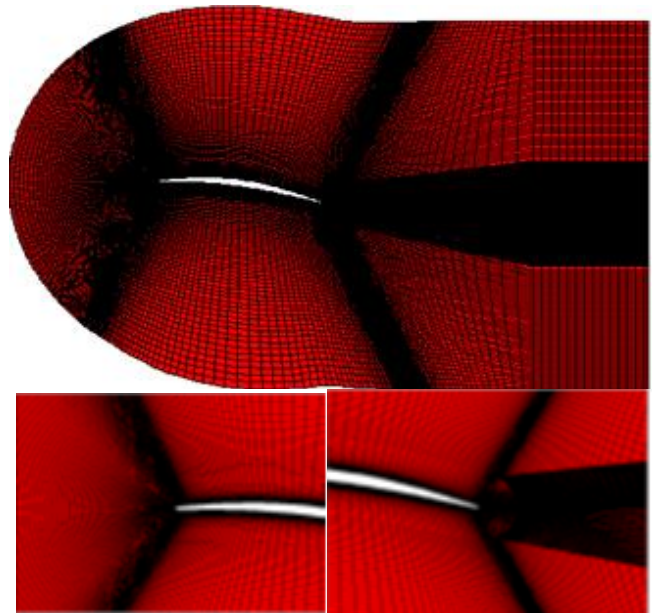
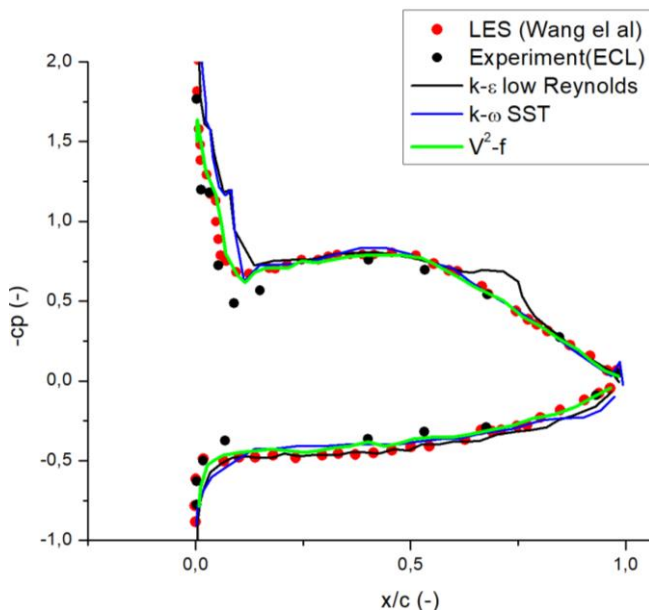


Figure 2: Refined mesh (86000 cells,  $0.15 < y^+ < 0.35$ )

## 5 Results and discussion

The simulation has been achieved by the last version of STAR-CD code, on a PC with two processors (2 CPU) and with a random memory of two Gigabits (2 GB). During the simulation, a mini cluster of 13 processors was helpful to complete the simulation (b21g,UMIST).

The comparison made between different models for the pressure coefficient shows a large recirculation captured by the k-ε model after half of the chord than the other models probably, due to the wrong turbulent energy estimation because of its limited wall function, the difference is obviously observed on the plots of the Figures 3 & 4. As well as, the reasonable agreement of the V<sup>2</sup>-f model due to its elliptic singularity function based on the normal velocity fluctuations comparing with the LES model and the experimental results (Ecole Central de Lyon).



**Figure 3:** Pressure coefficient at extrados and intrados of the airfoil

### 5.1 Turbulent energy

Although, the models V<sup>2</sup>-f, k-ω SST did not detect any turbulent zone at the trailing edge, but in comparison with these models and the LES model, the k-ε low Reynolds model indicates a high turbulent energy overestimation, which is an anomalous characteristic of the k-ε low Reynolds model near the separation zones. The plots on the Figure 5 represent a comparison of the kinetic turbulent energy for the different models.

Basing on the profiles shown in Figure 6, the validity of the V<sup>2</sup>-f model can be observed comparing with the LES model, as well as, a fast flow acceleration and increase of turbulent energy after the chord half for the k-ε model, which shown an overestimation of turbulent energy K near the trailing edge. The databases generated for the drawing profile of The Large Eddy Simulation (LES) calculated by the average value using a simple program developed in

FORTRAN language based on the turbulent energy fluctuation function:

$$K = \frac{1}{2}(\overline{u'^2} + \overline{v'^2} + \overline{w'^2}) \quad (6)$$

### 5.2 Prescribe velocity profile and turbulent intensity I in the Inlet flow

To check the probable causes of the turbulent energy overestimation observed on the k-ε low Reynolds model, an arbitrary turbulent intensity (I) has been introduced at the Inlet flow (Figure 6), with two different rates of the prescribe velocity (5%U, and 10%U), using a define function developed in FORTRAN language (bcdefi.f).

The plots of Figure 7 prove that the turbulent intensity has not any effects on the turbulent energy overestimation near the trailing edge zone. Therefore, the turbulent energy excess production near the trailing edge shown by the k-ε model are not due to the turbulent intensity at the Inlet flow.

## 6 Energy production expression

The production expression for the Low Reynolds k-ε model

$$P_k = \nu S_{ij} S_{ij} \quad (7)$$

The Strain

$$S = \sqrt{2S_{ij} S_{ij}} \quad (8)$$

The strain rate

$$S_{ij} = \frac{1}{2} \left( \frac{du}{dy} + \frac{dv}{dx} \right) \quad (9)$$

The first modification permits to replace the strain contribution by the multiplication of strain rate and the vorticity expression (LPM).

The vorticity:

$$\Omega_{ij} = \frac{1}{2} \left( \frac{\partial u}{\partial y} - \frac{\partial v}{\partial x} \right) \quad (10)$$

New production expression becomes

$$P_k = \nu S_{ij} \Omega_{ij} \quad (11)$$

The second modification permits to take the lowest value between the strain contribution and the multiplication of the strain rate and the vortices, in order to improve the production expression (Limiter Model):

$$P_k = \nu \min(S_{ij} S_{ij}, S_{ij} \Omega_{ij}) \quad (12)$$

Figure 8 shows the turbulent kinetic energy profiles obtained by the first modification LPM and compared to the LES and the standard k-ε models. The results indicate an overestimation of the turbulent kinetic energy far from the profile wall.

The velocity profiles in the Figures 9 & 10 show the effect of the linear turbulence production expression. We find that the limiter model provides a better agreement with the LES and the V<sup>2</sup>-f model, than the first modifications LPM.

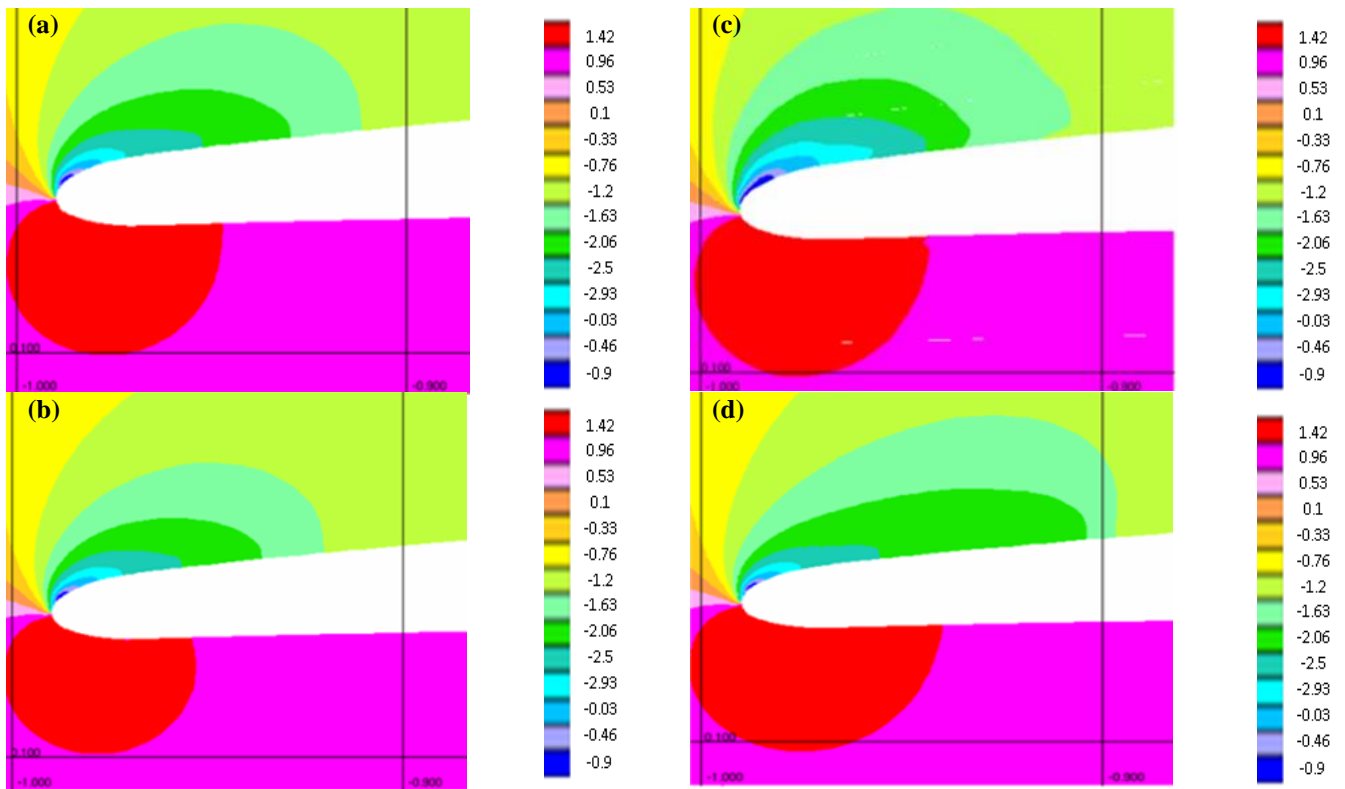


Figure 4: Pressure coefficient for: (a)  $V^2$ - $f$  model; (b)  $k$ - $\omega$  SST model; (c) LES model [7]; (d)  $k$ - $\epsilon$  low Reynolds model.

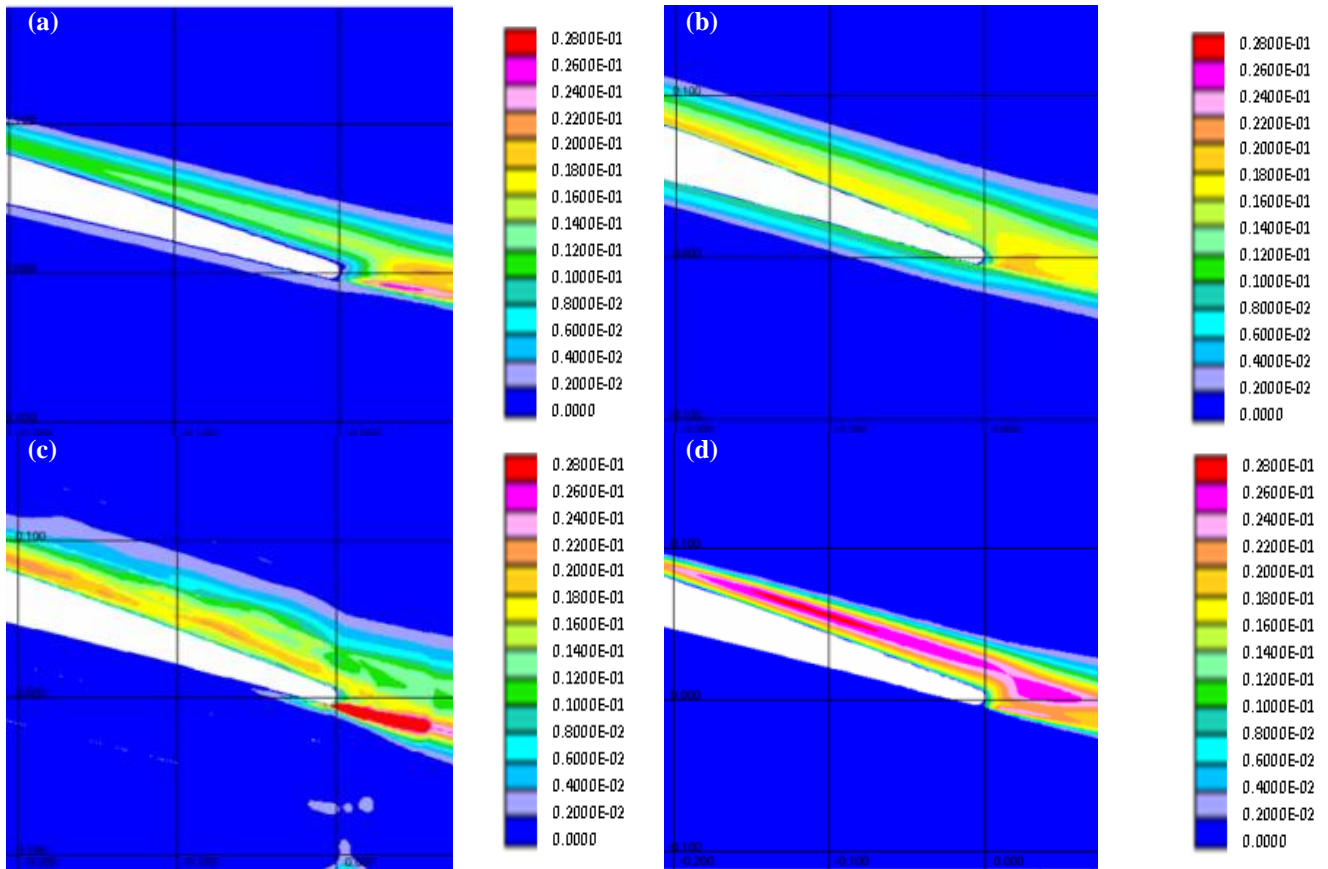
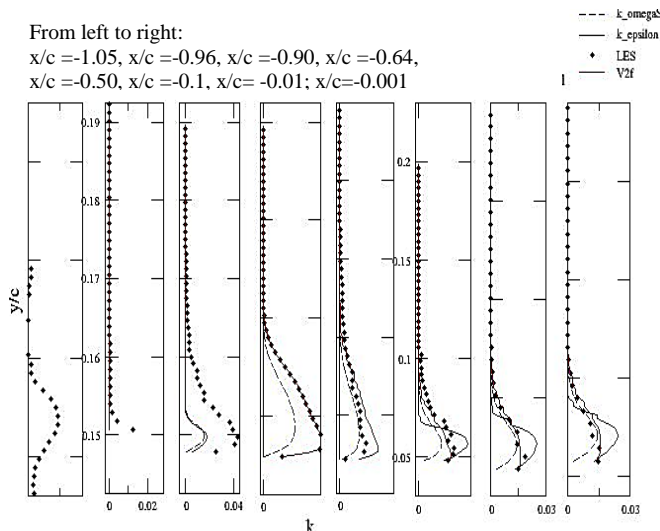
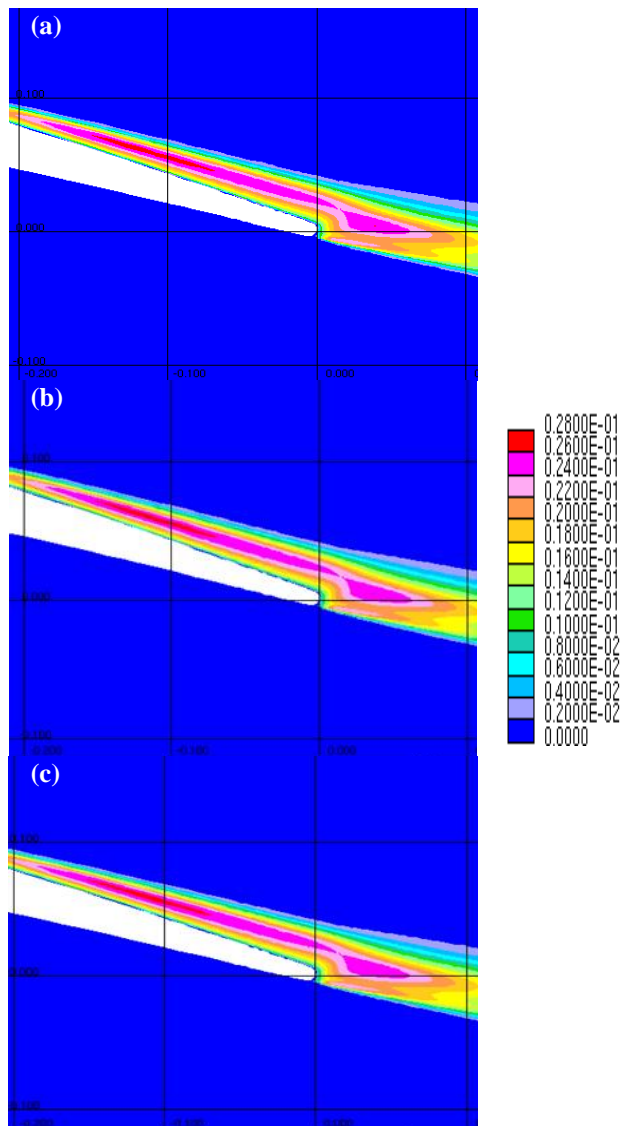


Figure 5: Kinetic turbulent energy at the trailing edge for: (a)  $V^2$ - $f$  model; (b)  $k$ - $\omega$  SST model; (c) LES model [7]; (d)  $k$ - $\epsilon$  low Reynolds model.



**Figure 6:** Turbulent energy profiles along the aerofoil chord for:  $k-\omega$  SST;  $k-\epsilon$ ; LES [7] &  $V2f$  model.



**Figure 7:** Turbulent energy: (a) without turbulent Intensity  $I$ ; (b)  $I=5\%U$ ; (c)  $I=10\%U$ .

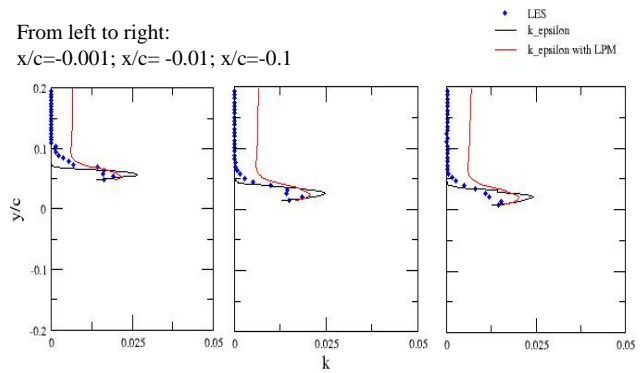


**Figure 8:** Turbulent kinetic energy profiles with the first modification LPM.

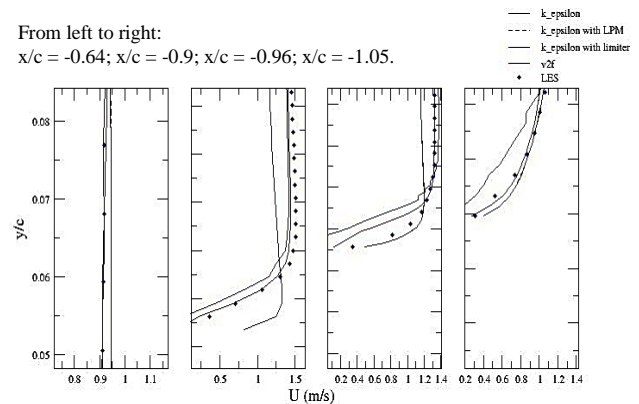


**Figure 9:** The Velocity profiles for the  $k-\epsilon$  model introducing Kato-Launder modifications LPM, and Limiter Model (treating edge).

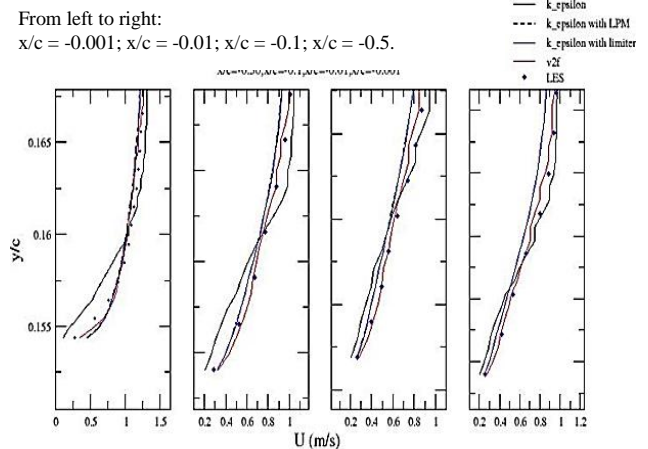


**Figure 10:** The Velocity profiles for the  $k-\epsilon$  model introducing Kato-Launder modifications LPM, and Limiter Model (leading edge)

The results in the figure 11 show that the modified  $k-\epsilon$  model confirm a better agreement with the experimental data than the standard  $K-\epsilon$  low Reynolds model. Hence, the prediction of the turbulent energy is improved near both zones leading and trailing edge. The observed improvements can be explained by the limitation of the turbulent energy production term that introduces the minimum between the vorticity and strain, as well as, the

corrected explicit damping function, particularly, near the separation zone (near wall corrections) which is based on a minimum dimensionless distance  $y^+$ . (About 0.35 in our case).

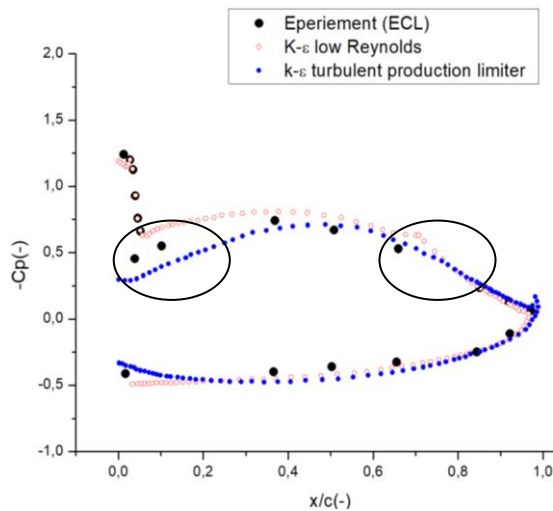


**Figure 11:** The pressure coefficient distribution obtained by the modified  $K-\epsilon$  model with comparison to the standard low Reynolds  $k-\epsilon$  model results and experimental data.

## 7 Conclusion

The model  $V^2-f$  represents a future solution basing on its high capacity of prediction for the turbulent energy phenomenon than the available RANS viscous models.

The insufficiency of the  $k-\epsilon$  low Reynolds model can be improved by replacing the strain rate by the vorticity in the turbulent energy production term, and correcting the explicit damping function near the separation zone. The comparison between the two modifications proved that the limiter model results are more stable than the first modification LPM.

Although the numerical investigation has been devoted to improve the estimation of the turbulent kinetic energy production, the improvement obtained can be useful to better predict the acoustic far field noise.

## Acknowledgments

The authors want to acknowledge the staff of the high school of Electrical Engineering and Energetic, for the help they provided to our work, particularly, the availability of the simulation tools, at the laboratory of fluid mechanics, as well as, the staff of the institute of aerospace and civil engineering MACE for their efforts for a best training and supervision.

## References

- [1]~M.J. Park, and D.J. Lee. Sources of broadband noise of an automotive cooling fan. 66-75, 2017.
- [2]~S. Moreau, G. Lacarino, S. Kang, Y. Khalighi, and M. Wang. Numerical simulation of a low speed fan blade. Proceedings of the CTR summer program., 195:207, 2012.
- [3]~M. Sanjosé, and S. Moreau. Direct numerical simulation of self noise of an installed control-diffusion airfoil., 39, 3:30,2011.
- [4]~S. Moreau. Influence of turbulent modelling on airfoil unsteady simulations of broadband noise sources: Valeo motors and Actuators. La Verière. France. Fred Mendonca. Science Direct. 2003.
- [5]~S. Moreau, M. Henner, G. Iaccarino, M. Wang, and M. Roger. Analysis of flow conditions in free jet experiments for studying airfoil self-Noise. AIAA Journal., 1895:1905, 2003.
- [6]~S. Moreau, M. Henner y, D. Casalino z, J. Gullbrand, G. Iaccarino, and M. Wang. Toward the prediction of low-speed fan noise. Center for turbulence research proceedings of the summer program, scaling properties of the aero-dynamic noise generated by low-speed fans. 2006.
- [7]~Y. Addad, D. Laurence, C. Talotte, and M.c. Jacob. Large eddy simulation of a forward backward facing step for acoustic source identification in Heat and fluid flow., 562:571, 2003.
- [8]~S. Montazeri, H. Kazemzadeh, and F. Bijan. Turbulent flow using a modified  $V^2-f$  turbulence model. IMECE2004., 587:594, 2004.
- [9]~G.~Iaccarino,~and~P.A~Durbin.~A~comparative asses-ment of the  $V^2-f$  model for recirculation flows. AIAA. 0765, 2003.,
- [10]~D.R. Laurence, J.C. Uribe, and S.V. Utyuzhnikov. A robust formulation of the  $V^2-f$  turbulence flow model and combustion., 169:185, 2004.
- [11]~L. Gaoa, J. Xua, and G. Gao. Numerical simulation of turbulent flow past airfoils on Open FOAM. Procardia Engineering., 756:761, 2012.
- [12]~J.B. Freund. Noise sources in a low Reynolds number turbulent jet at Mach 0.9. Fluid mechanics., 536:544, 2004.
- [13]~E. Ranjan, and R. Narasimha. Comparison of large eddy simulation and unsteady Reynolds-averaged Navier- Stockes for evaluation of entropy noise. Journal of fluids engineering., 1204-6, 2017.
- [14]~R. B. Kazerooni1, and S. K. Hannani. Mechanical engineering., 159:167, 2009.
- [15]~D. A. Anderson, J. C. Tannehill, and R. H. Pletcher. Computational fluid mechanics and heat transfer. Heimsphere Publishing Corporation, 1984.
- [16]~J.P. Caltagirone. Physique des écoulements continus. ERCOFTAC, 12-18, 2005.
- [17]~L. Blin. Modélisation statistique et simulation des grandes échelles des écoulements turbulents : application aux inverses de poussée. Université de Rouen. Science Direct, 15:21, 1999.

40 YEARS  
ANNIVERSARY

 **AcoustiGuard**<sup>®</sup>

**WILREP LTD.**

## SOUND and VIBRATION CONTROL



Since 1977, AcoustiGuard – WILREP LTD. has been providing products and solutions for sound and vibration control.

We are now pleased to announce the addition of our new **ARCHITECTURAL ACOUSTICS** product line.



Exclusive Canadian Dealer for RealAcoustix  
Exclusive North American Distribution of DeAmp and QuietStone

[www.acoustiguard.com](http://www.acoustiguard.com)

1-888-625-8944

**bquiet**  
SOUNDPROOF WINDOWS



It's that quiet.

**Cut down on noise and acoustic  
interference with Soundproof windows.**

**[www.bquiet.ca](http://www.bquiet.ca)  
1.877.475.9111**